Marine Chemistry 142-144 (2012) 29–40

Contents lists available at SciVerse ScienceDirect

Marine Chemistry

journal homepage: www.elsevier.com/locate/marchem

Distribution of sedimentary organic matter in estuarine–inner shelf regions of the East China Sea: Implications for hydrodynamic forces and anthropogenic impact

Limin Hu [a,*], Xuefa Shi [a], Zhigang Yu [b], Tian Lin [c,d], Houjie Wang [e], Deyi Ma [a], Zhigang Guo [d,e,**], Zuosheng Yang [e]

[a] Key Laboratory of Marine Sedimentology and Environmental Geology, First Institute of Oceanography, State Oceanic Administration, Qingdao 266061, China
[b] Key Laboratory of Marine Chemistry Theory and Technology, Ministry of Education, Ocean University of China, Qingdao 266100, China
[c] State Key Laboratory of Environmental Geochemistry, Institute of Geochemistry, Chinese Academy of Sciences, Guiyang 550002, China
[d] Department of Environmental Science and Engineering, Fudan University, Shanghai 200433, China
[e] College of Marine Geosciences, Ocean University of China, Qingdao 266100, China

ARTICLE INFO

Article history:
Received 19 April 2012
Received in revised form 19 August 2012
Accepted 21 August 2012
Available online 30 August 2012

Keywords:
Sources
Sedimentary organic matter
Hydrodynamic forces
Fate
Estuarine–inner shelf region of the ECS

ABSTRACT

The estuarine-inner shelf region of the East China Sea (ECS) is a major sink of the Yangtze River-derived fine-grained sediments and associated organic materials. In this work, surface sediment samples from a matrix of seventy-three sites that extend from the Yangtze River estuary (YRE) to the southern inner shelf were measured for their elemental, stable isotopic and molecular indices to provide a process-oriented study on the sources, distribution and fate of sedimentary organic matter (SOM) in this region. The results indicated that the re-suspension and alongshore transport of sediments could play a key role on the accumulation of SOM in the area. In addition to the physical reworking, the low C/N ratios and the enriched $\delta^{13}C$ values could also be likely related to the presence of microorganism-derived organic matter (OM) and soil-derived OM. The composition and principal component analyses of the *n*-alkanes indicated that the majority of the riverine terrigenous SOM was primarily restricted within the mud deposits along the coastal ECS. The wide occurrence and southward increasing trend of high molecular weight *n*-alkanes along the coastal ECS suggest an effective preferential dispersal of the terrigenous organic components. However, the local supply of the marine-derived OM potentially promotes the subsequent degradation of these terrigenous OM, which are likely responsible for the decreasing trend of the carbon preference index (CPI_{25-33}) from the northern YRE to the southern inner shelf. This indicates that the transported SOM from the YRE could become more homogenized as it moved toward the southern inner shelf. The presence of unresolved complex mixtures (UCM), lower Pr/Ph ratios and patterns of more stable geochemical biomarkers (hopanes and steranes) in the nearshore region reveals a petroleum contamination in the coastal environment.

1. Introduction

The coastal margins, especially the large river-influenced estuarine–coastal regions, are active interfaces between terrestrial and oceanic environments (Bianchi and Allison, 2009) that have a large discharge of fluvial materials, complex biogeochemical processes and anthropogenic inputs. Because more than 80% of global organic carbon burial occurs in these shallow marine systems, the sedimentary organic matter (SOM) in the coastal system serves an important role in the context of global carbon cycling (Berner, 1982; Hedges and Keil, 1995).

It has been reported that the burial of SOM in the dynamic estuarine–inner shelf area is complicated by different geological, hydrological and climatological settings (de Haas et al., 2002; Gordon and Goñi, 2003). Coastal hydrodynamic conditions can induce the rapid deposition, subsequent re-suspension and remobilization of sediments, which can significantly influence the quantity and type of buried organic matter (OM) in different depositional settings (Hedges et al., 1997; Bianchi et al., 2002; McKee et al., 2004; Hu et al., 2006; Zhu et al., 2008, 2011a). The efficient remineralization of SOM occurs during the frequent re-suspension of sediments (Aller, 1998). Therefore, a better examination of the origins, distribution and fate of SOM in sediments is essential to elucidate the mechanisms that control the preservation and cycling of SOM in dynamic coastal margins.

As one of the largest river-dominated marginal seas around the Chinese Mainland, the East China Sea (ECS) is primarily influenced by the Yangtze River (Bianchi and Allison, 2009) (Fig. 1), which has the world's fifth largest water discharge (944 km^3 yr^{-1}) and fourth largest sediment discharge at 480 Mt yr^{-1} (Yang et al., 2006). It has been indicated that the mud deposits in the Yangtze River estuary (YRE) and the inner shelf region are controlled by the seasonal changes of riverine input, estuarine processes, tidal currents, shelf circulation and storm/

* Corresponding author.
** Correspondence to: Z. Guo, Department of Environmental Science and Engineering, Fudan University, Shanghai 200433, China.
E-mail addresses: hulimin@fio.org.cn (L. Hu), guozgg@fudan.edu.cn (Z. Guo).

0304-4203/$ – see front matter © 2012 Elsevier B.V. All rights reserved.
http://dx.doi.org/10.1016/j.marchem.2012.08.004

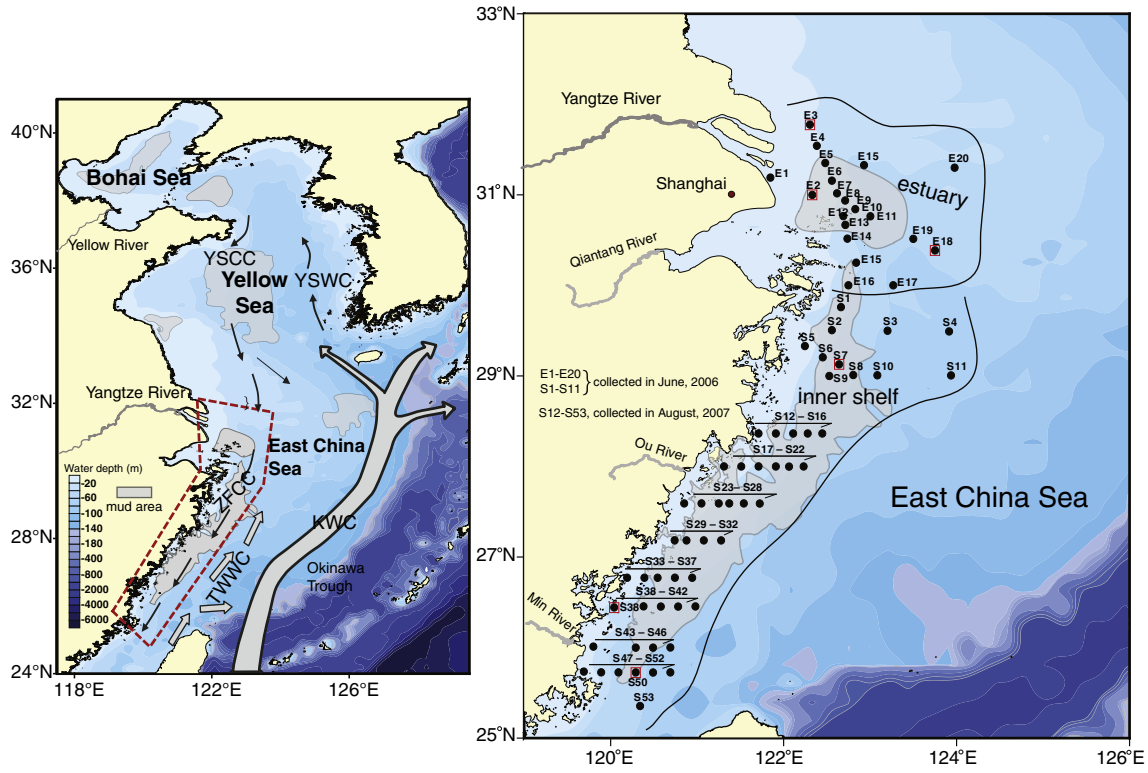

Fig. 1. Locations of the sampling sites and circulation systems in the ECS (Circulation systems and mud areas are modified according to Liu et al. (2007)). The red rectangle represents the stations that were chosen for the presentation of typical distribution diagram of *n*-alkanes in Fig. 4. KWC: Kuroshio Warm Current; TWWC: TaiWan Warm Current; ZFCC: Zhejiang–Fujian Coastal Current; YSCC: Yellow Sea Coastal Current; YSWC: Yellow Sea Warm Current.

typhoon episodes (Guo et al., 2003; Liu et al., 2007). Approximately 32% of the Yangtze-derived sediments are believed to be accumulated in the inner shelf (Milliman et al., 1985; Liu et al., 2007), while ~40% can be accounted for the sediments north of 30°N (DeMaster et al., 1985). Therefore, the majority of the Yangtze-derived sediments and associated OM are trapped within the estuarine–inner shelf area (Milliman et al., 1985; Yang et al., 1992; Liu et al., 2006). The hydrodynamics of the coastal ECS play an important role in the redistribution, transport and fate of these re-suspended sediments from the YRE to the southern inner shelf (Guo et al., 2003; Liu et al., 2007).

Previously, Kao et al. (2003) reported a close association between SOM with fine-grained sediments and the possible delivery of SOM from the inner shelf to the southern Okinawa Trough. The dispersal and distribution of terrigenous SOM under the control of depositional settings in the Lower Yangtze River–ECS shelf system have also been recently examined by Zhu et al. (2008, 2011a). Deng et al. (2006) suggested that the riverine discharge and upwelling of the Kuroshio intrusion are key factors for the burial of organic carbon over the shelf. More recently, Xing et al. (2011) identified the terrigenous and marine SOM in the ECS shelf using multi-proxies of biomarkers. Moreover, it was indicated that the recent anthropogenic impact such as the petroleum residue inputs could also influence the occurrence of SOM in the estuarine area (Bouloubassi et al., 2001).

However, the most samples in previous studies were beyond the range of the inner shelf region and/or with limited sampling sites covering the water depth <— 50 m. The study on the fate of SOM in the coastal ECS with a finer spatial sampling resolution covering the entire regime of the estuarine–inner shelf region is still limited. In addition, most samples in the earlier studies were collected before the implementation of the Three Gorge Dam (TGD) in 2003; therefore, the potential effect of dam construction on the SOM has been scarcely touched. In this work, seventy-three surface sediment samples covering the entire coastal ECS region with the finer spatial sampling resolution were measured for elemental, stable isotopic and molecular indices to present a comprehensive study on the sources, distribution and fate of SOM in the estuarine–inner shelf system of the ECS.

2. Materials and methods

2.1. Sample collection

The sampling sites are shown in Fig 1. The majority of the samples were collected from mud areas. The sediment samples of E1–E20 and S1–S11 were collected by the *R/V Dong Fang Hong 2* of the Ocean University of China in June 2006, and the remaining samples (S12–S53) were obtained by the *R/V Kan 407* in August 2007. Surface sediment samples (0–3 cm) were collected using a stainless steel box corer. The sediment samples were wrapped in aluminum foil and stored at −20 °C until analysis.

2.2. Analytical procedure

The grain sizes of the samples were determined using a laser particle size analyzer (Mastersizer 2000, Malvern Instruments Ltd., Malvern, Worcestershire, UK). The particle sizes were <4 μm for clay, 4–63 μm for silt and >63 μm for sand. The relative error in the particle sizes of duplicate samples was less than 3% (n = 6).

Portions of the freeze-dried sediment samples were decalcified using 4 M hydrochloric acid and subsequently rinsed with deionized water (3–4 times) before drying overnight at 60 °C. The resulting carbonate-free samples were then analyzed for total organic carbon (TOC) and total nitrogen (TN) in duplicate using a Vario EL-III Elemental Analyzer, and the average values were reported (Hu et al., 2009). Replicate analyses of one sample (n = 6) provided a precision of ±0.02 wt.% for TOC and ±0.005 wt.% for TN. Stable carbon isotope analysis of the organic carbon was performed on the carbonate-free

samples using a Thermo Delta^{plus} XL mass spectrometer operating in continuous flow mode, according to the procedure of Hu et al. (2009).

The organic analyses were performed at the State Key Laboratory of Organic Geochemistry. The procedures for the extraction and fractionation of the aliphatic hydrocarbons followed those described by Hu et al. (2009). Briefly, hydrocarbons were extracted from the freeze-dried and pulverized sediment samples (15–20 g) with dichloromethane (DCM) in a Soxhlet apparatus for 48 h, and activated copper was added to remove sulfur. The extracts were then reduced, hexane-exchanged and separated on the 1:2 alumina: silica gel glass column. The target fraction containing the aliphatic and polyaromatic hydrocarbon fraction was eluted with 15 ml of hexane and 20 ml of 1:1 (v/v) hexane: dichloromethane. Hexamethylbenzene was added to the extract as an internal standard, and the mixture was concentrated to 0.2 ml and injected into an Agilent 6890 Series Gas Chromatograph/Series 5975 Mass Spectrometer (GC/MSD) operating in the full scan mode. The GC/MSD was equipped with a DB-5MS capillary column (30 m × 0.25 mm i.d., 0.25 μm film thickness, J&W Scientific) and helium was used as the carrier gas (1.0 ml min^{-1}). Samples were injected in the split-less mode with an injector temperature of 280 °C. The oven temperature was programmed to increase from 60 °C to 180 °C (1 min hold) at a rate of 8 °C min^{-1} and from 180 °C to 300 °C (2 min hold) at a rate of

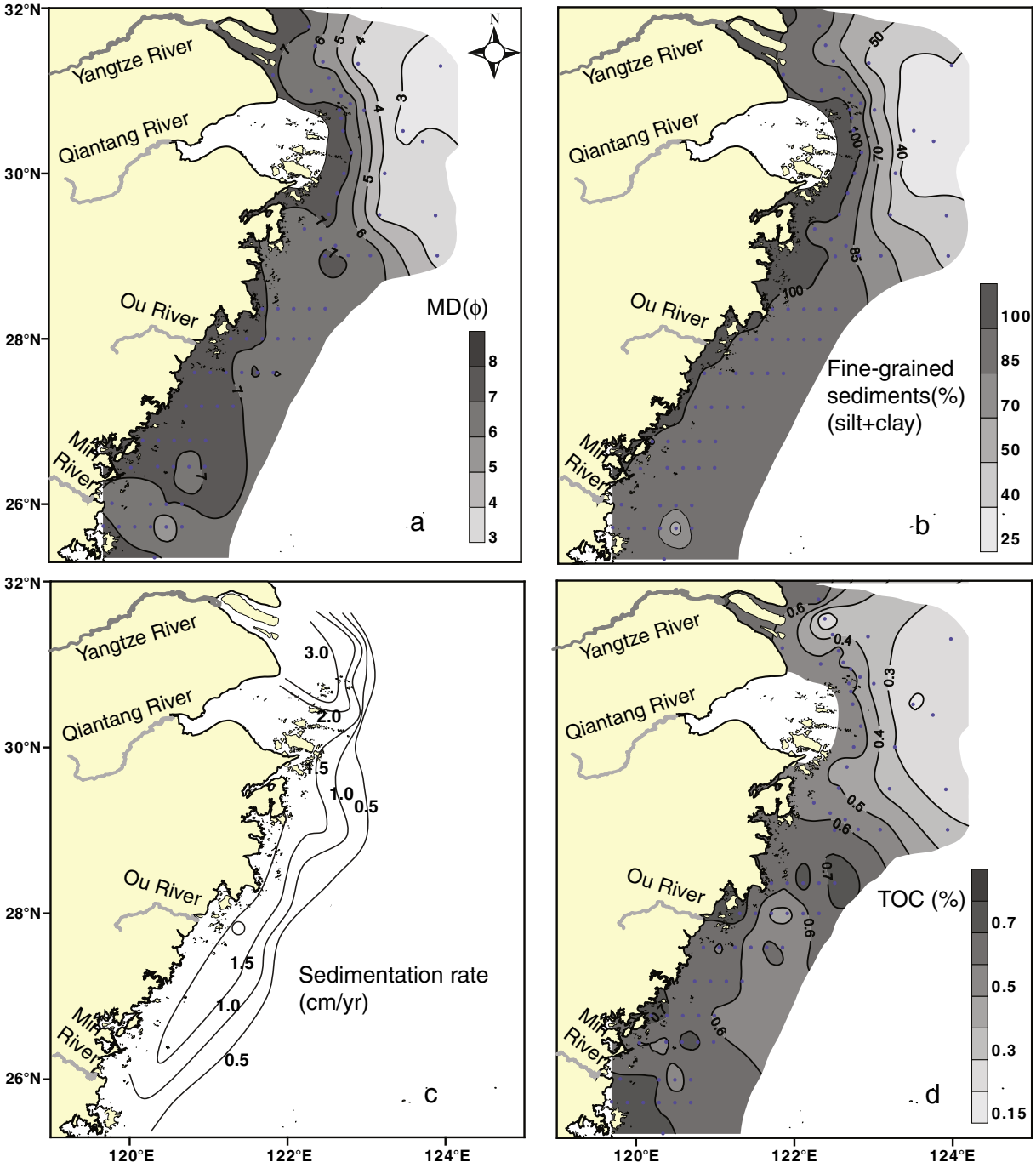

Fig. 2. Distributions of the median diameters (MD) of the sediments, fine-grained sediment fractions, sedimentation rates and TOC content in the surface sediments from the estuarine–inner shelf region.
The distribution of sedimentation rates along the coastal ECS was redrawn from Liu et al. (2006).

3 °C min^{-1}. The mass spectrometer was operated in the electron impact (EI) mode (70 eV) with a scanning range between *m/z* 50 and 500. Detection of the hopanes and steranes was performed by monitoring for their typical ions: *m/z* 191 for hopanes and *m/z* 217, 218 for steranes.

The quantification of *n*-alkanes were based on authentic standards containing (C_{12}, C_{14}, C_{16}, C_{18}, C_{20}, C_{22}, C_{24}, C_{26} and C_{28}), and the hexamethylbenzene was added to the extract prior to instrument analysis as the internal standard. The corresponding relative response factors of these authentic standard compounds of alkanes (C_{12}–C_{28}) to the internal standard were calculated accordingly (five-point calibration). A surrogate standard (phenanthrene-d_{10}) was added to the samples before extraction, and recoveries of 86.2 ± 12.3% were obtained. Procedural blanks and standard spiked blanks were also evaluated and showed no noticeable interference.

2.3. Principal component analysis (PCA)

PCA, a multivariate analytical tool, was used to determine the distribution of the samples and to study the relationships of the measured parameters. Before analysis, the non-detectable values were replaced with concentration values equal to one-half of the method detection limits. Then, the raw data matrix was Z-scoring standardized and mid-range normalized to eliminate the influence of the different units and to ensure that each determined variable had equal weighting in the PCA. PCA was performed using the program *SPSS 13.0* for Windows (SPSS Inc., Chicago, IL, USA).

3. Results and discussion

3.1. The grain-size distribution of surface sediments and background depositional setting

As shown in Fig. 2a and b, fine-grained sediments (silt and clay) were predominant in the YRE and inner shelf, showing a narrow band that extends southward along the inner-most part of the shelf with a finer median grain size (6Φ − 7Φ), whereas the outer region off the YRE was primarily characterized by a relatively coarser particle size (<5Φ) with a higher sand fraction (>55%). The reported ^{210}Pb chronologies indicated that high accumulation rates (>3 cm/yr) occurred immediately adjacent to the YRE subaqueous delta, then decreased southward alongshore and eastward offshore (Liu et al., 2006) (Fig. 2c). Generally, the most fluvial sediments from the Yangtze River are temporarily deposited in the estuarine system (YRE subaqueous delta) during the flood season from June to October (Guo et al., 2003; Liu et al., 2006) while the coastal current is weakened in the summer due to the prevailing southeast monsoon. However, driven by the wind-induced waves in the winter, the initially deposited sediments in the estuarine systems are readily re-suspended and transported southward along the inner shelf by the Zhejiang–Fujian coastal current (ZFCC). This unique sedimentary process could greatly influence the dispersal and fate of the Yangtze-derived fine-grained sediments and associated materials in the coastal ECS (Guo et al., 2003; Liu et al., 2006, 2007; Hu et al., 2011a).

3.2. Distribution and sources of SOM

3.2.1. TOC-based parameters

The TOC contents in the samples ranged from 0.17% to 0.82% with a mean of 0.57%. The average TOC content in the samples from the YRE mud areas (0.55%) was relatively lower than that from the southern inner shelf (0.64%, Table 1). This corresponded to the southward increasing trend of fine-grained constituents (Fig. 2d), suggesting the potential influence of hydrodynamic forces on the accumulation of SOM and sediment sorting in the coastal ECS.

It has been reported that marine-derived OM has a C/N ratio between 5 and 7, whereas terrigenous OM typically has a C/N ratio greater than 15 (Redfield et al., 1963; Meyers, 1997). As shown in Table 1, the C/N ratios (wt/wt) in the sediment samples from the estuary and inner shelf ranged from 9.01 to 13.44 and from 4.98 to 12.12, with a mean of 10.88 and 7.23, respectively. Generally, the observed low C/N ratios in this study were compared to those in other river-dominated depositional regions around the world, such as the Bohai Sea (average C/N = 6.6, Hu et al., 2009), the Mississippi estuary and adjacent area (average C/N = 6.4, Bianchi et al., 2002), the Ayeyarwady continental shelf (C/N mostly ranged between 6 and 8, Ramaswamy et al., 2008) and the Amazon shelf (average C/N = 6.5, Showers and Angle, 1986). The lowing C/N ratios could be primarily attributed to anthropogenic influences and/or natural causes, for example, the preferential sorption of inorganic N by minerals (Müller, 1977; Schubert and Calvert, 2001; Hu et al., 2006), soil-derived OM (Hedges and Oades, 1997; Ramaswamy et al., 2008) and/or microorganism origin (Ruttenberg and Goñi, 1997; Hu et al., 2009; Xing et al., 2011). Nevertheless, according to the close correlation between TOC and TN (Fig. 3a), the positive TOC intercept (i.e. the negative TN intercept) in correlation plots (especially for the samples from the inner shelf) suggested that there was a mixture of N-rich OM pool with extremely N-poor pool of OM (e.g. terrestrial organic matter), thus, the sorption of inorganic N cannot account for the low C/N ratio in the coastal ECS as reported in the Amazon shelf region (Ruttenberg and Goñi, 1997). Recently, Zhu et al. (2011b) reported that the riverine branched GDGTs (Glycerol dialkyl glycerol tetraether) (tetraether lipids) degraded more extensively in the YRE, which are therefore hypothesized to track the labile fraction of soil OM in this setting. This provides a potential evidence for the presence of microorganism-derived OM in the present work since soil microbes are nitrogen rich with dominated bacterial and fungal populations (Hedges and Oades, 1997). Therefore, the low C/N ratios observed in this study could be likely due to the presence of microorganism-derived OM, which is also readily enhanced by the winnowing or re-suspension of the fine-grained sediments and anthropogenic inputs (e.g., petroleum residues, see below) in the coastal setting (Ruttenberg and Goñi, 1997; Hu et al., 2011b).

Furthermore, the samples from the southern inner shelf had lower C/N ratios than those in the YRE (Table 1), indicating a more presence of marine-derived OM. It is also reported that the soil-derived OM adsorbed onto fine fraction can selectively transport out of the estuarine area along the main sediment dispersal system (Tesi et al., 2007). Considering the potential sediment sorting caused by the physical reworking as noted above, the preferential alongshore transport of fine-grained sediments in the coastal ECS with more non-woody

Table 1
Parameters of bulk organic matter and sediment grain size of the surface sediments in the estuary area and southern inner shelf.

Sediment samples		TOC (%)	C/N	$\delta^{13}C$ (‰)	Sand (%)	Silt (%)	Clay (%)	Md (Φ)
Estuarine area (n = 20)	Range	0.17–0.70	9.01–13.44	−24.62 to −20.61	0.32–73.01	16.83–70.92	8.16–36.07	2.51–7.34
	Average	0.44 ± 0.16	10.88 ± 1.05	−22.31 ± 1.17	21.49	54.21	24.3	5.78 ± 1.68
Southern inner shelf (n = 53)	Range	0.25–0.82	4.98–12.12	−22.52 to −21.05	0.07–54.84	27.86–83.74	14.73–35.56	3.68–7.35
	Average	0.64 ± 0.12	7.23 ± 1.79	−22.05 ± 0.44[a]	6.65	66.89	26.51	6.71 ± 0.88

[a] The $\delta^{13}C$ of the samples (n = 16) from the southern inner shelf were partially based on Kao et al. (2003).

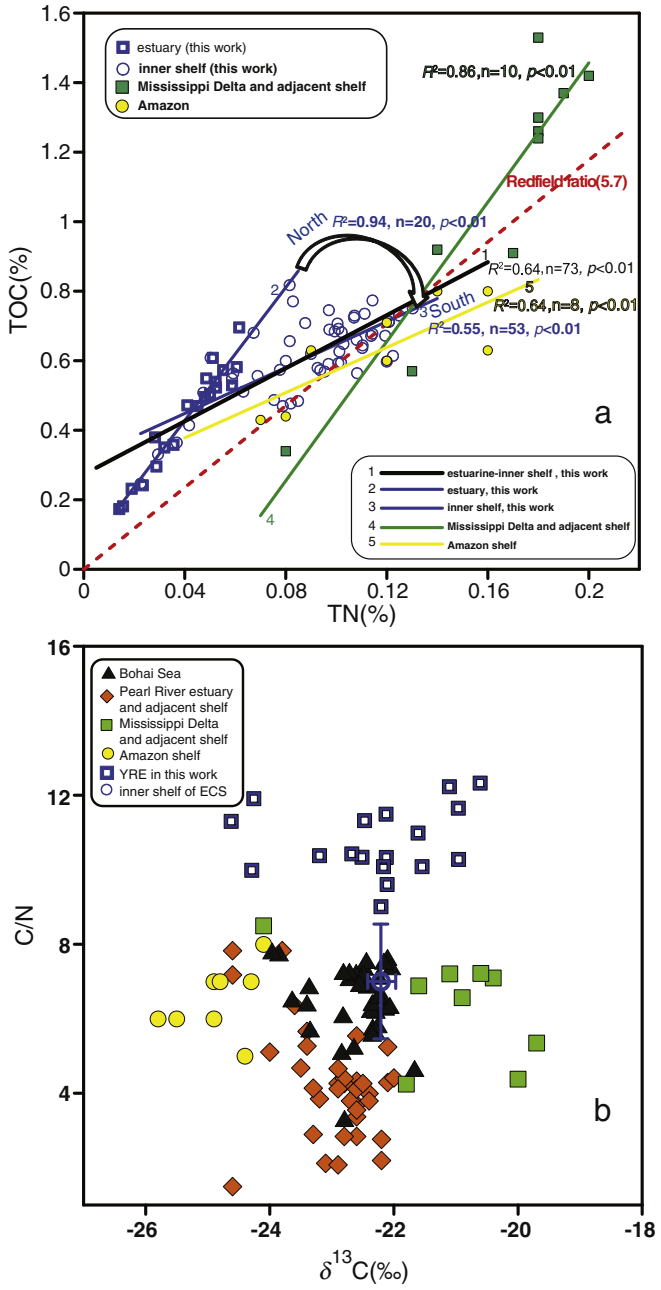

Fig. 3. (a) The scatter plot of TOC and TN in the surface sediment samples from the estuary and inner shelf of ECS and comparing with other river dominated margins around the world. Redfield ratio of 5.7 (wt/wt) is shown in red dashed line. (b) $\delta^{13}C$ and C/N bio-plot of surface sediments in the coastal ECS and comparing with other river-dominated margins around the world such as Amazon shelf (Showers and Angle, 1986); Mississippi Delta and adjacent shelf (Bianchi et al., 2002); Pearl River estuary (Hu et al., 2006) and Bohai Sea (Hu et al., 2009). The samples from the inner shelf are shown by one outline circle with error bar.
Partially data from Kao et al. (2003).

biogenic (see below) and soil-derived OM could also be responsible for the obvious southward decreasing gradient of the C/N ratios (Fig. 3a). This indicates that the re-suspension and alongshore transport of sediments could be not only responsible for the accumulation of SOM but also play a role in the elemental signature of SOM in this region.

The bulk organic carbon isotope composition ($\delta^{13}C$) is another index for identifying the sources of SOM. Marine OM typically has $\delta^{13}C$ values ranging from −19‰ to −21‰ (Fry and Sherr, 1984). Terrestrial plants with a C_3 pathway have an average $\delta^{13}C$ value of −27‰ (−22‰ to −33‰), whereas the ratio ranges from −9‰ to −16‰ with a mean of −13‰ for the C_4 pathway (Pancost and Boot, 2004). The $\delta^{13}C$ value in the majority of the estuarine samples in this study ranged from −24.6‰ to −20.6‰, which is similar to that of suspended OM (−25.4‰ to −19.7‰) in the YRE (Tan et al., 1991), but depleted than those from the ECS continental shelf (−22.7‰ to −20.1‰) (Xing et al., 2011). The C_4 plant OM contribution for the SOM in the coastal ECS should be minimal since the particulate organic carbon (POC) of the Yangtze are dominated by C_3 plant (Wu et al., 2007), and the relative proportion of the C_3 plant contribution in the samples from the estuary and southern inner shelf area was estimated as 83% and 95%, respectively (Guo et al., 2006). Therefore, the modern terrestrial OM discharged by the Yangtze River into the coastal ECS is mainly derived from C_3 land vascular higher plants. For the samples from the inner shelf, Kao et al. (2003) reported a smaller and narrower range of $\delta^{13}C$ values (−22.5‰ to −21.9‰), which indicates an increasing fraction of marine-derived OM. Likewise, as shown in Fig. 3b, the $\delta^{13}C$ values in the coastal ECS were observed to be comparable to those from the Huanghe River estuary and its adjacent Bohai Sea (−23.9‰ to −22.5‰) (Hu et al., 2009) and the Pearl River estuary and its adjacent shelf (−24.6‰ to −22.0‰) (Hu et al., 2006) but slightly enriched compared to those from the Amazon shelf (−25.8‰ to −24.1‰). It is found that the majority of the $\delta^{13}C$ values in the Gulf of Mexico are relatively more enriched than the others (Fig. 3b), which could be related to the river-borne C_4 plant components from the watershed (Ruttenberg and Goñi, 1997), potentially reflecting the different climatic region and the drainage basin characteristic of other large rivers around the world. In fact, except for the C_4 plant OM contribution, the soil-derived OM and fertilization are also found to be responsible for the enriched $\delta^{13}C$ in samples derived from farming fields (O'Leary, 1985; Hedges and Oades, 1997), the relatively enriched $\delta^{13}C$ in the coastal ECS could be thus partially related to the agricultural inputs in addition to the more recent increased anthropogenic influence by the rapid urbanization, industrialization and reclamation in the drainage basin as those similar evidence from the Pearl River delta and estuary (Yu et al., 2010). Therefore, the agricultural inputs of soil-derived OM and potential anthropogenic influence could also be factors influencing the elemental and isotopic compositions of the bulk SOM in the estuarine–inner shelf system in addition to the physical reworking disturbance.

3.2.2. Aliphatic hydrocarbons

Normal alkanes (*n*-alkanes), ranging from C_{14} to C_{35}, occurred in all samples with an almost 10-fold range of concentration levels, from 0.44 to 4.31 μg g^{-1} (dry weight) (Table 2). As shown in Fig. 4, there was a strong odd to even carbon preference in the high molecular weight (HMW) *n*-alkanes ($\geq C_{25}$) in the YRE samples (e.g. sites E2, E3, and E18) with C_{max} at C_{31}, suggesting a prominent terrigenous contribution from higher vascular plant wax. The increased proportion of low molecular weight (LMW) *n*-alkanes in the samples from the southern inner shelf (e.g. sites S7, S38, and S50) indicates an increased amount of marine-derived OM. The presence of unresolved complex mixtures (UCM, mainly branched and cyclic hydrocarbons) as shown in Fig. 4 indicates the anthropogenic inputs of petroleum hydrocarbons (Bouloubassi et al., 2001). The observed bimodal presence with high concentrations of short chain alkanes along the southern coast (sites S7 and S50) (Fig. 4) is likely related to the presence of microbial biodegradation potentially enhanced by the recent fossil fuel inputs (Aboul-Kassim and Simoneit, 1996; Hu et al., 2009).

The relative proportion of the terrestrial and marine contributions for *n*-alkanes is usually measured from the terrigenous/aquatic ratios (TAR) as $(C_{27}+C_{29}+C_{31})/(C_{15}+C_{17}+C_{19})$ (Meyers, 1997), even though this method may overestimate the terrigenous inputs because of the preferential preservation of terrestrial hydrocarbons over their planktonic counterparts (Volkman et al., 1987). As shown in Fig. 5, higher TAR values (>6) and elevated carbon preference index

Table 2
Concentrations of *n*-alkanes and hydrocarbon parameters for surface sediments in the estuary area and southern inner shelf.

Sediment samples		*n*-ALK	TAR	ALKter%	CPI_{25-33}	Pr/Ph	*m/z* 191		*m/z* 217
		($\mu g\ g^{-1}$)					Ts/(Ts+Tm)	αβ C_{31} S/(S+R)	ααα C_{29} (S/(S+R))
Estuarine area (n=20)	Range	0.44–3.76	0.9–12.3	20.4–61.4	3.09–6.15	1.12–2.77	0.14–0.45	0.39–0.59	0.35–0.68
	Average	1.83±0.89	4.5±2.9	46.9±12.1	4.58±0.95	1.74±0.50	0.32	0.54	0.56
Southern inner shelf (n=53)	Range	0.49–4.31	1.8–20.5	30.5–67.6	2.59–5.42	0.85–3.69	0.12–0.51	0.45–0.58	0.50–0.69
	Average	2.67±0.76	7.7±4.0	52.8±8.5	3.95±0.65	1.66±0.57	0.43	0.53	0.63

n-ALK: total concentration of *n*-alkanes (C_{14} to C_{35}); TAR: terrigenous/aquatic ratio: $(nC_{27}+nC_{29}+nC_{31})/(nC_{15}+nC_{17}+nC_{19})$ (Meyers, 1997); ALKter%: the percentage of the "terrigenous *n*-alkanes (C_{27}, C_{29}, C_{31}, and C_{33})"; CPI_{25-33}: carbon preference index = (1/2) $[(nC_{25}+nC_{27}+nC_{29}+nC_{31}+nC_{33})/(nC_{24}+nC_{26}+nC_{28}+nC_{30}+nC_{32})+(nC_{25}+nC_{27}+nC_{29}+nC_{31}+nC_{33})/(nC_{26}+nC_{28}+nC_{30}+nC_{32}+nC_{34})]$ (calculated as Aboul-Kassim and Simoneit, 1996); Pr/Ph: ratio of pristane to phytane; Ts: 18α(*H*)-22,29,30-trisnorhopane; Tm: 17α(*H*)-22,29,30-trisnorhopane.

(CPI_{25-33}) were mainly restricted within the river mouth and the inner-most area along the coast. The higher TAR observed in the nearby coast in the Min River estuary could reflect a local dominant fluvial contribution. The sum of these most abundant *n*-alkanes (C_{27}, C_{29}, C_{31} and C_{33}) related to biogenic terrigenous origins is referred to as "terrigenous *n*-alkanes" (ALKter), accounting for 20–67% of the total *n*-alkanes with more than 56% encountered in the alongshore mud deposits extending southward (Table 2 and Fig. 5b). The concentration of *n*-alkanes and percentage of the "terrigenous *n*-alkanes" (ALKter%) in the present study was compared to those previously reported in the YRE (0.16 to 1.88 $\mu g\ g^{-1}$ with the ALKter% of 40–60%) before the implementation of the TGD (Bouloubassi et al., 2001). Therefore, the concentration and composition of *n*-alkanes in the estuarine samples did not differ significantly in recent years after the implement of TGD although with a ~60% reduced annual sediment load during 2003–2006 (Yang et al., 2006). The insignificant alteration of sedimentary *n*-alkanes in the estuary could be explained as the following points: (1) the decrease of sediment load could have a more impact on the flux of terrigenous *n*-alkanes rather than on their concentrations and/or compositions in the estuarine area; (2) the surface sediment samples in the present study were collected in 2006 and 2007, only 3–4 years after the first impounding water and sediment discharge in 2003. The upper deposits of samples (0–3 cm) are still likely reflecting the occurrence of SOM around the 2003 and/or 2004. Therefore, the significant alteration of the terrigenous OM input caused by the TGD could be hardly archived only based on the surface sediment samples; (3) the extensive physical reworking disturbance and alongshore transport of sediments as noted above is also likely masking the information of the alteration of terrigenous OM inputs. Moreover, recent studies showed that the operation of TGD in 2003 had a more impact on the delivery of OC by suspended particulate matter (SPM) in the middle reach than in the lower reach and estuary area; the contributions of the tributaries and lakes were enhanced in the lower Yangtze River (Yu et al., 2011). On the other hand, as response to the influence of TGD, it is also observed that significant channel erosion has occurred in the downstream (Yang et al., 2007; Xu and Milliman, 2009) with the reduction of primary production and changing of nutrient ratio in the coastal ECS (Gong et al., 2006).

Phytane (Ph) is essentially absent in the uncontaminated recent sediments, and a high concentration of pristane (Pr) can be derived from zooplankton and some other marine animals (Volkman et al., 1992), which results in a higher Pr/Ph ratio (typically between 3 and 5). However, a Pr/Ph value close to or less than 1 suggests petroleum contamination (Gao and Chen, 2008). As shown in Fig. 5d, the relatively low Pr/Ph ratios (<1.5) were mainly constrained to samples from the YRE and the Zhejiang and Fujian coasts in the south, implying an

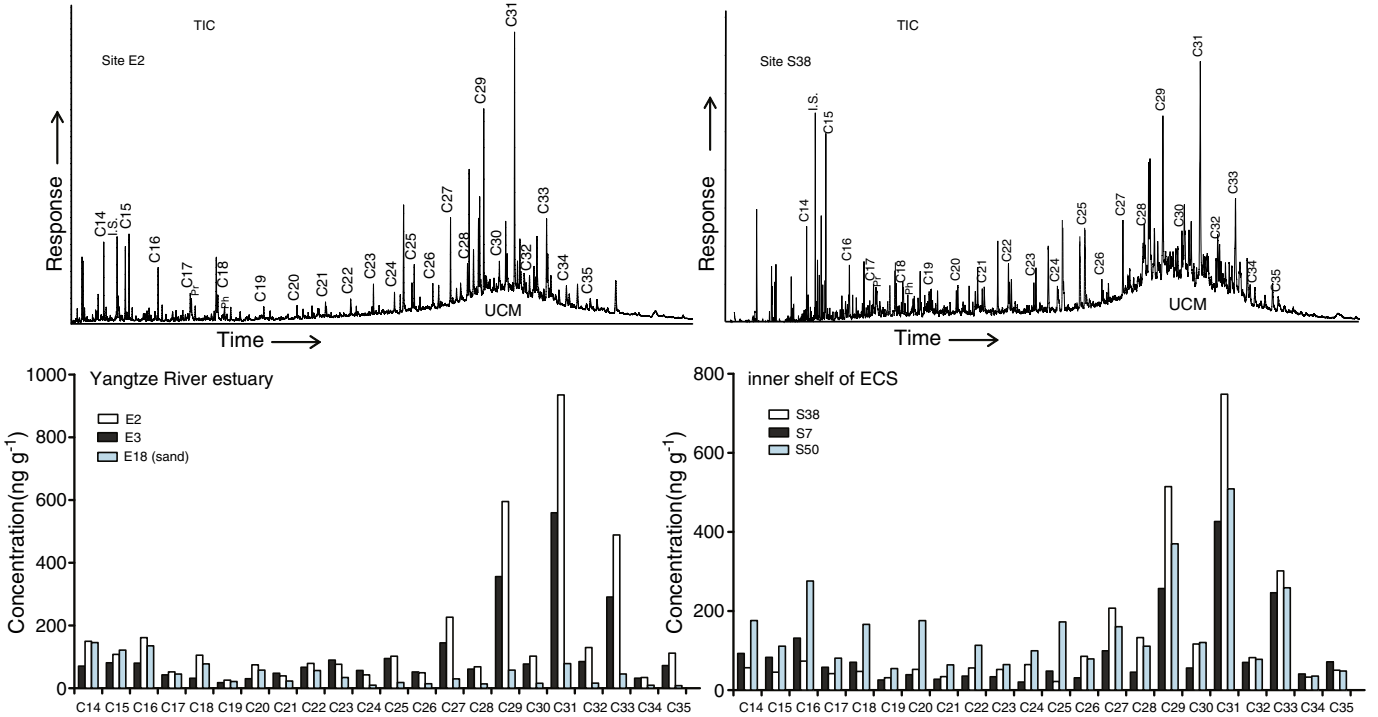

Fig. 4. GC–MS chromatograms of the aliphatic hydrocarbons in sediment samples at sites E2 and S38 and typical histogram of *n*-alkanes concentrations and composition patterns in the sediment samples from the coastal ECS (These selected stations were labeled in Fig. 1 by the red rectangle).

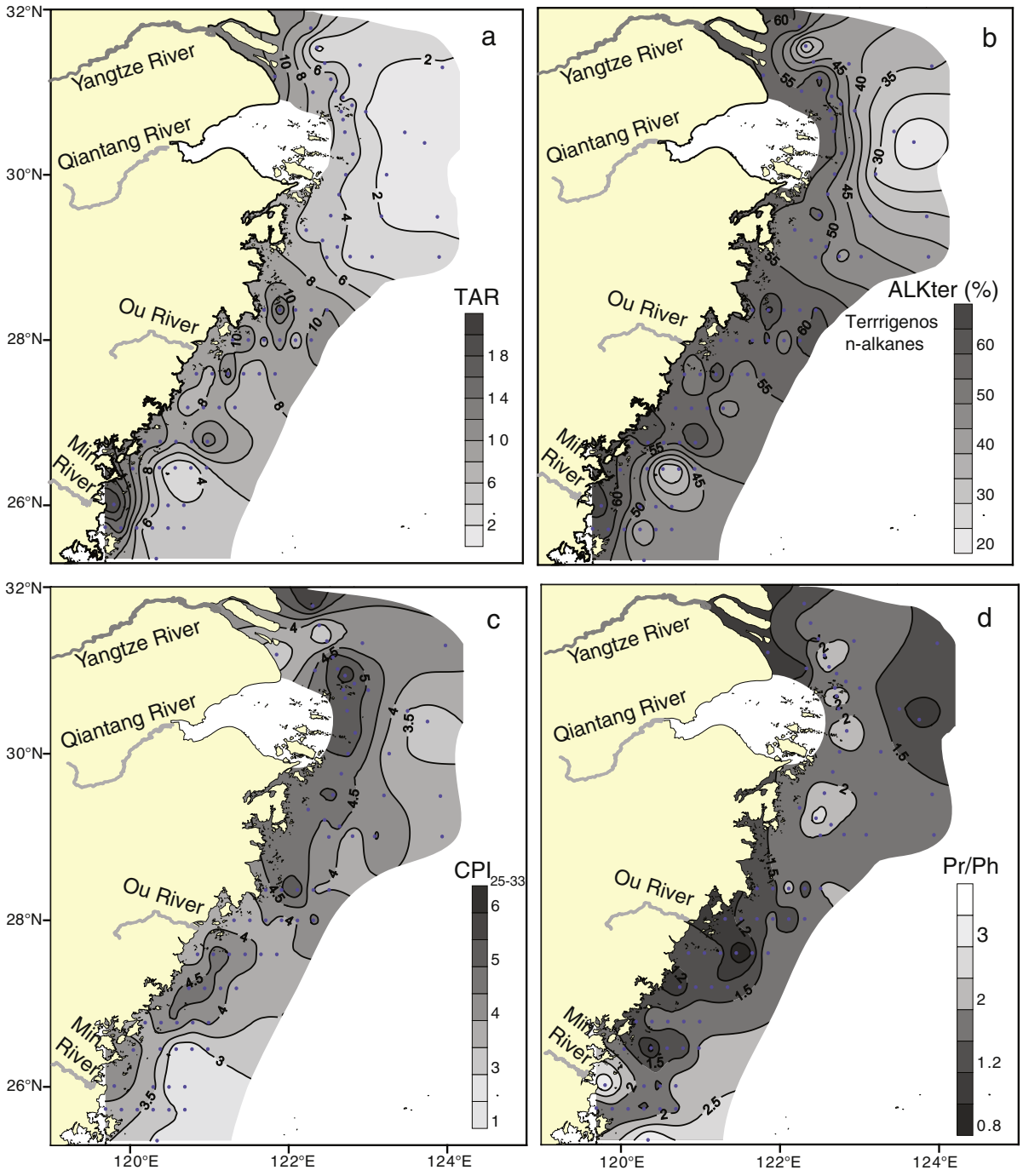

Fig. 5. Distribution of *n*-alkane-based parameters in the surface sediments from the coastal ECS. (a) TAR, (b) ALKter(%), (c) CPI_{25-33} and (d) Pr/Ph.

anthropogenic input of petroleum residues likely due to the local river discharge and shipping activities.

3.2.3. Identification of SOM sources using principal component analysis (PCA)

By performing PCA on the datasets, including the individual *n*-alkanes, TOC, TN and sediment grain size, the scree plot of eigenvalues indicated that 84% of the data variance could be explained by the first four principal components (PCs) (Fig. S1), and the first two principal components (PC1 and PC2) was shown to explain 71% of the total data variance (Fig. 6a and Table S1). PC3 only explained 8% of the total variance which was insignificant correlated with these individual variables except for the C_{15} and C_{35} (Table S1). There is no reasonable interpretation or reference to support this factor. Therefore, we mainly focus on the first two components in the present study.

As shown in Fig. 6, PC1, which accounting for 52% of the data variance, was distinguished by the most individual *n*-alkanes, TOC and fine-grained sediments with high positive loading, while the sand constituent was evident with negative loading. Considering the large river-dominated setting, PC1 could be mainly attributed to fluvial terrigenous OM input although there is some mixture with LMW *n*-alkanes. PC2 explained 19% of the total data variance, which was mainly characterized by the positive loading of LMW *n*-alkanes and negative loading of HMW *n*-alkanes, revealing the contribution of marine-derived OM (Fig. 6a). The higher positive loadings of individual *n*-alkanes and the fine-grained sediments on PC1 indicate that the mud area in the coastal area is the main sink for the SOM. Furthermore, the presence of the even

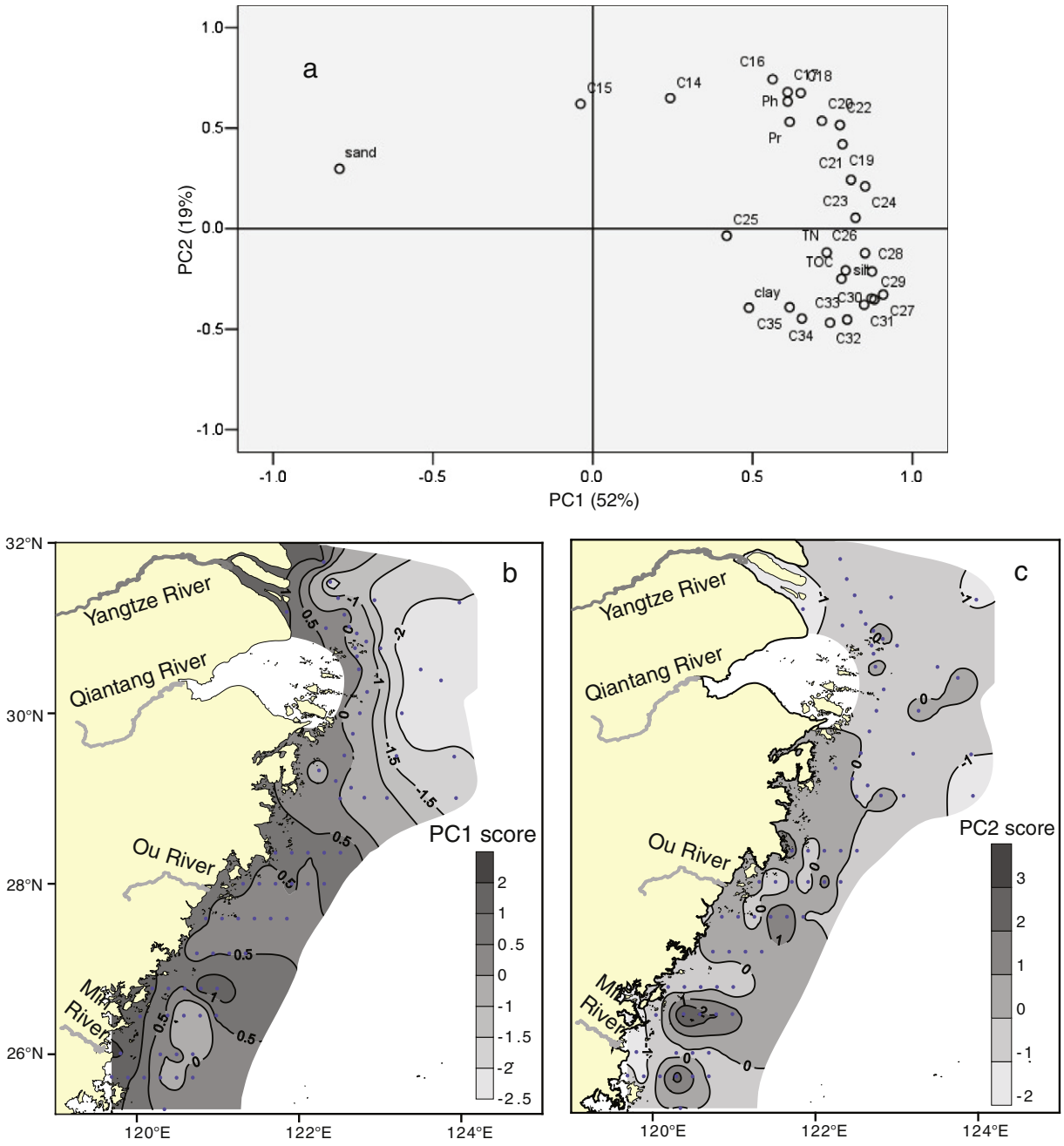

Fig. 6. Loading plot of PCA (a) and the spatial patterns of the corresponding sample scores from PC1 (b) and PC2 (c).

carbon *n*-alkanes (C_{14}, C_{16}, and C_{18}), Pr and Ph on PC2 indicates that they could be primarily derived from algal, bacterial and/or petroleum sources (Gao and Chen, 2008).

As shown in Fig. 6b and c, the group of samples with higher PC1 scores was restricted to the river mouth and the inner-most area along the coasts, indicating a major terrigenous contribution. The samples in the inner shelf region with co-existing LMW *n*-alkanes and high positive score on PC2 are primarily related to a more recent contribution of marine-derived OM, suggesting a continuous local supply of planktonic materials to the alongshore transport system with extensive diagenetic fractionation (Aller, 1998; Blair and Aller, 2012). Furthermore, the addition of these newly produced and highly reactive marine biogenic substances (e.g., plankton, microbial biomass) and their mixing within the re-suspended and transported SOM pools could also potentially promote the decomposition and remineralization of the terrestrial-derived OM possessing more refractory matrix (Aller et al., 1996; Blair and Aller, 2012). This probably lowers the CPI_{25-33} in the sediment samples from the southern inner shelf region (Fig. 7), and could potentially enhance the bottom oxygen depletion in the water column (Chen et al., 2007).

3.3. Implication for the hydrodynamic forces and river inputs on the fate of SOM

According to the selected typical offshore-transects (lines 1–5) from the estuarine–inner shelf region, it can be observed that HMW *n*-alkane concentrations and CPI_{25-33} values significantly decreased from the coast towards the open area along the estuarine offshore-transects (lines 1–2), where TOC showed a close correlation with the sediment grain size (Fig. 7). This observation suggests the dominance of fluvial terrigenous OM inputs, which could also be attributed to the rapid co-deposition of these fluvial sediments and their associated land-

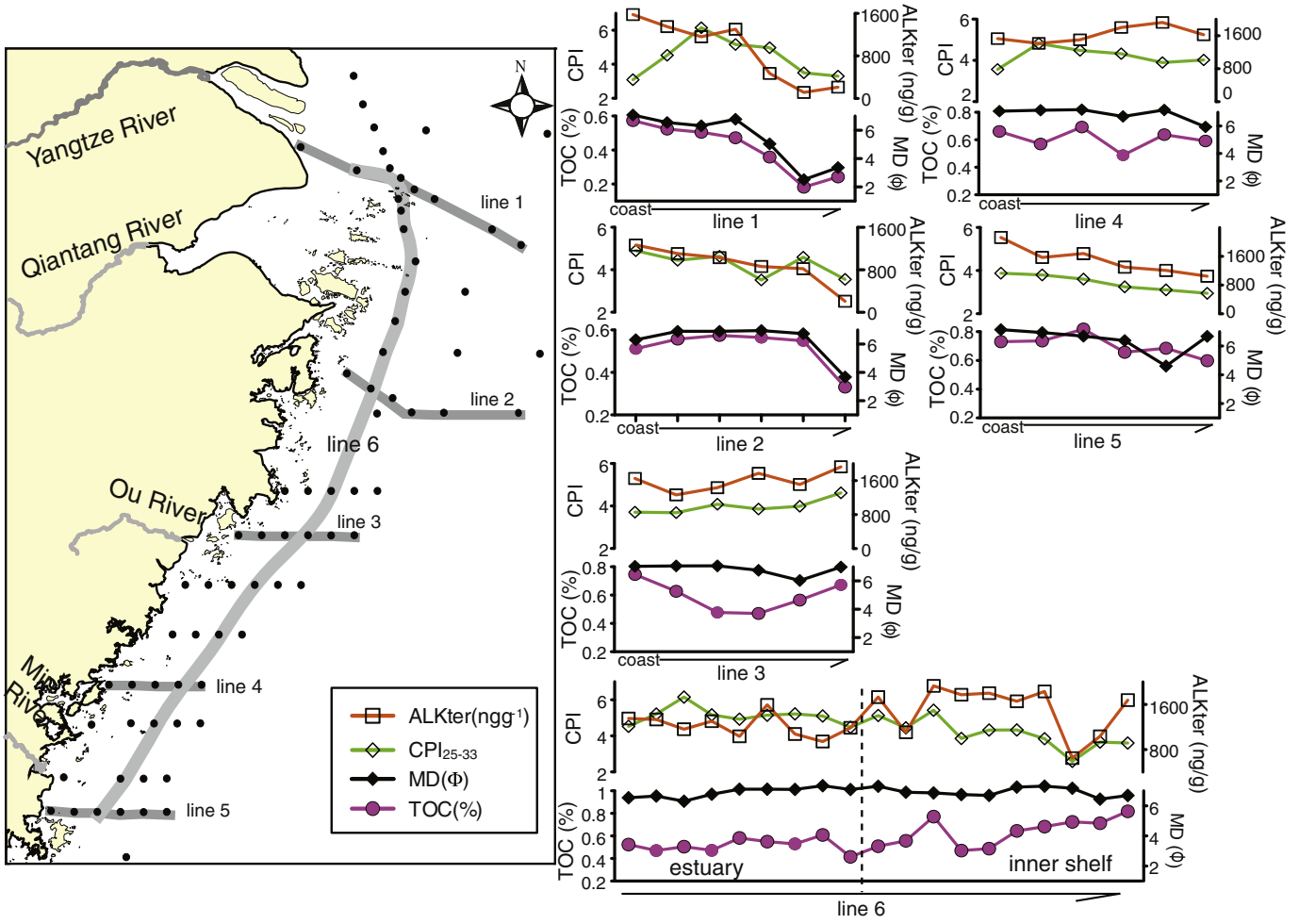

Fig. 7. Distribution of TOC, median diameters, CPI_{25-33} and HMW *n*-alkane concentrations in the offshore (lines 1–5) and alongshore transects (line 6) in the coastal ECS.

based organic components caused by the gravitational sedimentation and/or coagulation in the river-sea mixing zone (DeMaster et al., 1985; Hu et al., 2011a). However, for the southern offshore-transects (lines 3–5) in the inner shelf, the absence of the offshore decreasing gradient for HMW *n*-alkanes and TOC is potentially due to the closer proximity to the coast (Fig. 1), indicating that the majority of the fine-grained sediment-associated fluvial OM are mainly restricted within the estuarine and inner-most area of the shelf region.

However, for the alongshore-transect (Line 6) from the estuarine area in the north to the inner shelf in the south (Fig. 7), TOC and HMW *n*-alkanes showed increasing trends with a higher fraction of fine-grained constituent (e.g., clay component) from the YRE to the southern inner shelf, which reflects a more grain size dependence on the aggregation of terrigenous *n*-alkanes. Actually, it has been well-documented that the biogenic components of non-woody vascular plants (i.e., lignin-poor), including *n*-alkanes, are more easily associated with fine silt and clay and therefore, are preferentially transported away from the estuary to the distal mud deposits, whereas the lignin-rich coarser woody debris is mostly deposited in the estuary and inshore areas (Prahl et al., 1994; Bianchi et al., 2002; Zhu et al., 2008). Moreover, the terrestrial molecular components of the SOM characteristically degrade less rapidly than their marine counterparts (Zonneveld et al., 2010; Blair and Aller, 2012). This could be responsible for the wide occurrence of HMW *n*-alkanes, especially in the river-dominated coastal ECS under the extensive hydrodynamic sorting conditions. Such hydrodynamic sorting increases the proportion of the fine-grained constituents and non-woody biogenic components along the southward dispersal system, which in turn disturb the elemental and isotopic signatures of SOM as mentioned above. Therefore, a more effective dispersal and accumulation of the terrigenous organic materials with refractory matrix of land-based constituents should exist during the re-suspension and transport of fine-grained sediments. Furthermore, as noted in the PCA, the mixing of local supply of planktonic materials with these transported SOM from the YRE could also potentially promote the decomposition and remineralization of the terrestrial-derived OM. This implies that the more heterogeneous SOM initially re-suspended from the estuarine system could become more homogenized as it moves towards the southern inner shelf.

3.4. Anthropogenic impact and chemical fingerprinting of biomarkers for petroleum contamination

As noted above, the anthropogenic impacts have been reflected by the potential disturbance on the elemental and isotopic signature of OM as well as the composition of molecular markers (e.g. Pr/Ph, UCM and CPI_{25-33}). However, these indices still cannot provide a solid evidence for the specific anthropogenic source, such as the presence of petroleum inputs.

The hopanes and steranes in sediments are mainly converted from their corresponding biogenic precursors, and these stable geochemical biomarkers could provide more convincing evidences for petroleum contamination and have been widely used to detect petroleum pollution and identify its source in estuarine and coastal systems (Hostettler et al., 1999; Bouloubassi et al., 2001). The representative mass fragmentograms of *m/z* 191 (hopanes) and 217 (steranes) from the sediment samples in the coastal ECS are shown in Fig. 8a.

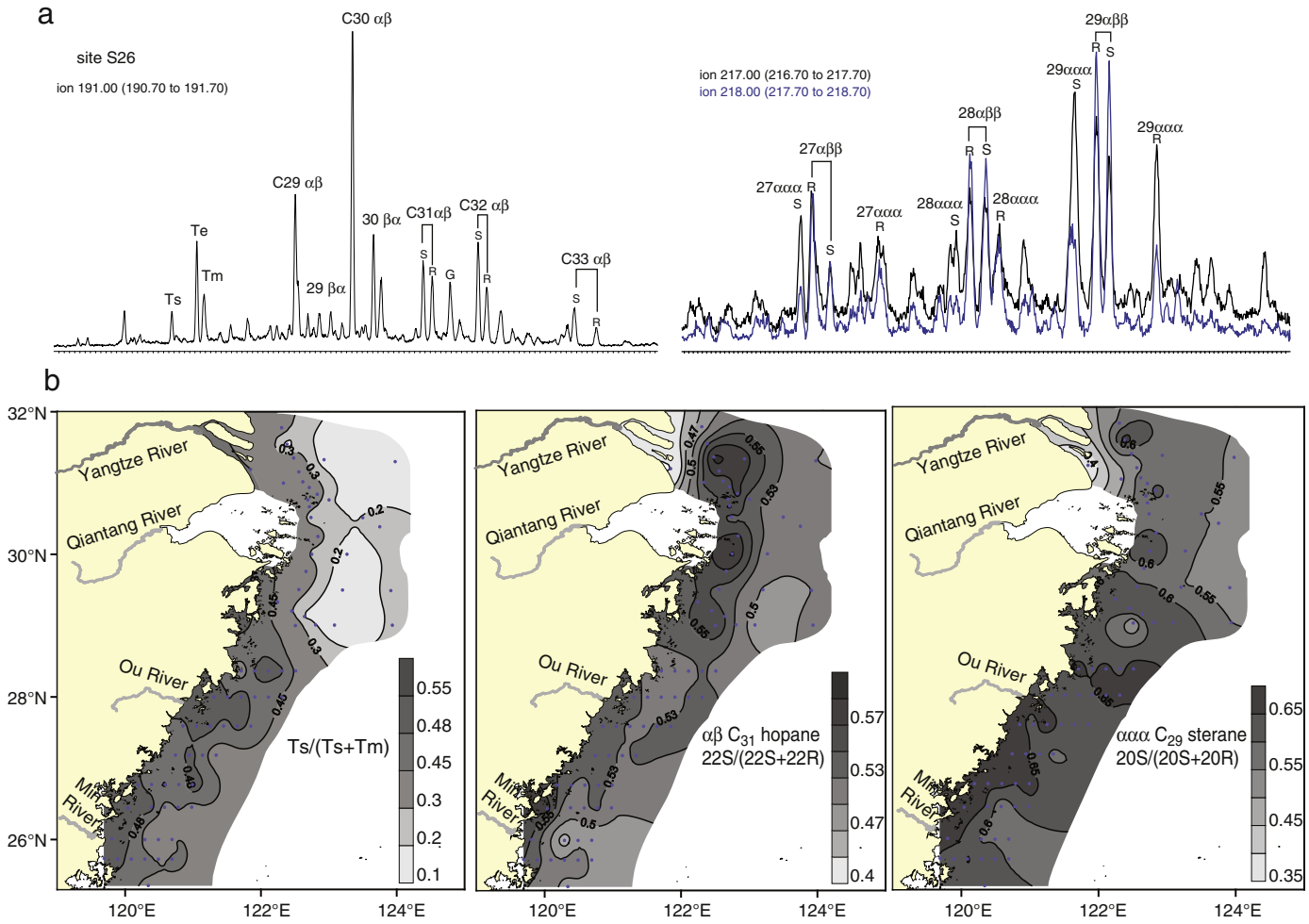

Fig. 8. (a) Typical mass fragmentogram of *m/z* 191 (hopanes) and *m/z* 217 (steranes) from the sediment samples from the coastal ECS; (b) spatial distribution patterns of the Ts/(Ts+Tm), homohopanes S/(S+R) and ratios of C_{29} sterane S/(S+R). (α, β=17α (H), 21β (H)-hopanes; β, α=17β(H), 21α(H)-hopanes; G = gammacerane; Ts=18α(H)-22,29,30-trisnorhopane; Tm=17α(H)-22,29,30-trisnorhopane; Te=17β(H)-22,29,30-trinorhopene; αααα=5α(H), 14α(H), 17α(H)-steranes; αββ=5α(H), 14β(H), 17β(H)-steranes; R and S=C-22 R and S configurations).

The hopanes comprised a series of 17α (H), 21β (H)-compounds (C_{27}–C_{34}), maximizing at the C_{30} homologue with less prominent 17β (H), 21α (H)-hopanes (Fig. 8a). The Ts/(Ts+Tm) ratios (Ts= 18α-22,29,30-trisnorhopane, Tm=17α-22,29,30-trisnorhopane) and the 22S/(22S+22R) epimers of the homohopanes have been used to characterize the origin and the degree of maturation of crude oil (Hostettler et al., 1999). The relative content of Ts is higher in the more stable and mature homologues as demonstrated in the crude oil and mature sedimentary rocks, whereas the equilibrium value of the fully mature homohopane S/(S+R) usually occurs at 0.6 (Mackenzie, 1984). In this study, the Ts/(Ts+Tm) ratios in the samples ranged broadly from 0.12 to 0.51, and for homohopane, S/(S+R) varied from 0.39 to 0.59, (Table. 2). As shown in Fig. 8b, the observed higher homohopane S/(S+R) ratios in the samples from the estuarine and southward mud deposits were accompanied by the relatively lower Pr/Ph (<1.5) ratios with the presence of UCM (Fig. 4). This suggests the presence of mature petroleum hydrocarbon inputs. Gammacerane, as a biomarker commonly found in most Chinese crude oil geologically derived from lacustrine sources (Fu and Sheng, 1989) was also present in the samples as shown in Fig. 8. Similar hopane distributions were also reported in the other Chinese petroleum samples from Shengli Oilfield (Pang et al., 2003) and sediment samples from the Bohai Sea (Bigot et al., 1989; Hu et al., 2009).

The patterns of steranes detected in the samples were comprised mainly of the 5α, 14β, 17β- and 5α, 14α, 17α-configurations occurring as the 20S and 20R epimers with a maximum at the C_{29} homologue (Fig. 8a). Values of αααα C_{29} sterane S/(S+R) ratios in the sediment samples ranged from 0.35 to 0.69 (Table 2) (close to the equilibrium value of 0.55), suggesting the presence of mature constituents in the surface intervals (Aboul-Kassim and Simoneit, 1996). The enhanced occurrence of the C_{29} homologue is typical of non-marine petroleum such as crude oil from China as reported before (Fu and Sheng, 1989; Bouloubassi et al., 2001). As shown in Fig. 8b, the higher ratio values of the C_{29} sterane S/(S+R) were mainly observed in the southern nearshore samples along the Zhejiang–Fujian provinces, which is likely due to the closer proximity to the coast with more land-based petroleum inputs through the coastal rivers and surface runoff as well as the heavy shipping activities.

4. Conclusions

The increasing proportions of fine-grained constituents and non-woody biogenic components along the southward dispersal system could provide evidences that hydrodynamic forces influence the sediment sorting and accumulation of SOM in the coastal ECS. Moreover, the presence of microorganism-derived organic matter and anthropogenic inputs could also be responsible for the low C/N ratios and enriched $\delta^{13}C$ in the coastal ECS. The abundance of HMW *n*-alkanes with higher CPI_{25-33} values and PCA results suggest the dominance of fluvial terrigenous OM inputs from the Yangtze River

into the estuarine region with a local supply of newly planktonic-derived OM in the southern inner shelf. The preferential dispersal and accumulation of the terrigenous OM with refractory matrix of land-based constituents could be responsible for the homogenization of the transported SOM during the dispersal system under a potential subsequent degradation induced by the local addition of marine-derived OM. Anthropogenic input of petroleum hydrocarbon is revealed by the presence of UCM, lower Pr/Ph ratios and compositional patterns of the more stable geochemical biomarkers (hopanes and steranes) in the nearshore region.

Acknowledgments

This work was supported by the Natural Science Foundation of China (NSFC) (No. 40920164004), the State Oceanic Administration (SOA), China (Nos. GY02-2012G08 and 2012312) and the NSFC (Nos. 41076015 and 41103046); and also in part by China Postdoctoral Science Foundation funded project (No. 20110491626). We wish to thank the crew of the *R/V Dong Fang Hong 2* and of the *Kan 407* for collecting the sediment samples. The anonymous reviewers and editors (Frank J. Millero and Gay Ingram) should be sincerely appreciated for their constructive comments and suggestions that greatly improved this study.

Appendix A. Supplementary data

Supplementary data to this article can be found online at http://dx.doi.org/10.1016/j.marchem.2012.08.004.

References

Aboul-Kassim, T.A.T., Simoneit, B.R.T., 1996. Lipid geochemistry of surficial sediments from the coastal environment of Egypt I. Aliphatic hydrocarbons — characterization and sources. Mar. Chem. 54 (1–2), 135–158.
Aller, R.C., 1998. Mobile deltaic and continental shelf muds as suboxic, fluidized bed reactors. Mar. Chem. 61 (3–4), 143–155.
Aller, R.C., Blair, N.E., Xia, Q., Rude, P.D., 1996. Remineralization rates, recycling, and storage of carbon in Amazon shelf sediments. Cont. Shelf Res. 16 (5–6), 753–786.
Berner, R.A., 1982. Burial of organic carbon and pyrite sulfur in the modern ocean: its geochemical and environmental significance. Am. J. Sci. 282, 451–473.
Bianchi, T.S., Allison, M.A., 2009. Large-river delta-front estuaries as natural "records" of global environmental changes. Proc. Natl. Acad. Sci. 106, 8085–8092.
Bianchi, T.S., Mitra, S., McKee, B.A., 2002. Sources of terrestrially-derived organic carbon in lower Mississippi River and Louisiana shelf sediments: implications for differential sedimentation and transport at the coastal margin. Mar. Chem. 77 (2–3), 211–223.
Bigot, M., Saliot, A., Cui, X., Li, J., 1989. Organic geochemistry of surface sediments from the Huanghe estuary and adjacent Bohai Sea (China). Chem. Geol. 75 (4), 339–350.
Blair, N.E., Aller, R.C., 2012. The fate of terrestrial organic carbon in the marine environment. Annu. Rev. Mar. Sci. 4 (1), 401–423.
Bouloubassi, I., Fillaux, J., Saliot, A., 2001. Hydrocarbons in surface sediments from the Changjiang (Yangtze River) estuary, East China Sea. Mar. Pollut. Bull. 42 (12), 1335–1346.
Chen, C.C., Gong, G.C., Shiah, F.K., 2007. Hypoxia in the East China Sea: one of the largest coastal low-oxygen areas in the world. Mar. Environ. Res. 64 (4), 399–408.
de Haas, H., van Weering, T.C.E., de Stigter, H., 2002. Organic carbon in shelf seas: sinks or sources, processes and products. Cont. Shelf Res. 22 (5), 691–717.
DeMaster, D.J., McKee, B.A., Nittrouer, C.A., Jiangchu, Q., Guodong, C., 1985. Rates of sediment accumulation and particle reworking based on radiochemical measurements from continental shelf deposits in the East China Sea. Cont. Shelf Res. 4 (1–2), 143–158.
Deng, B., Zhang, J., Wu, Y., 2006. Recent sediment accumulation and carbon burial in the East China Sea. Global Biogeochem. Cycles 20 (3), GB3014.
Fry, B., Sherr, E.B., 1984. $\delta^{13}C$ measurements as indicators of carbon flow in marine and freshwater ecosystems. Mar. Sci. 27, 13–47.
Fu, J.M., Sheng, G.Y., 1989. Biological composition of typical source rocks and related oils of terrestrial origin in the People's Republic of China, a review. Appl. Geochem. 4, 13–22.
Gao, X., Chen, S., 2008. Petroleum pollution in surface sediments of Daya Bay, South China, revealed by chemical fingerprinting of aliphatic and alicyclic hydrocarbons. Estuarine Coastal Shelf Sci. 80 (1), 95–102.
Gong, G.C., et al., 2006. Reduction of primary production and changing of nutrient ratio in the East China Sea: effect of the Three Gorges Dam? Geophys. Res. Lett. 33 (7), L07610 http://dx.doi.org/10.1029/2006gl025800.
Gordon, E.S., Goñi, M.A., 2003. Sources and distribution of terrigenous organic matter delivered by the Atchafalaya River to sediments in the northern Gulf of Mexico. Geochim. Cosmochim. Acta 67 (13), 2359–2375.
Guo, Z.G., Yang, Z.S., Fan, D.J., Pan, Y.J., 2003. Seasonal variation of sedimentation in the Changjiang estuary mud area. J. Geogr. Sci. 13, 348–354.
Guo, Z.G., Li, J.Y., Feng, J.L., Fang, M., Yang, Z.S., 2006. Compound-specific carbon isotope composition of individual long-chain *n*-alkanes in severe Asian dust episodes in the North China coast in 2002. Chin. Sci. Bull. 51, 2133–2140.
Hedges, J.I., Keil, R.G., 1995. Sedimentary organic matter preservation: an assessment and speculative synthesis. Mar. Chem. 49 (2–3), 81–115.
Hedges, J.I., Keil, R.G., Benner, R., 1997. What happens to terrestrial organic matter in the ocean? Org. Geochem. 27 (5–6), 195–212.
Hedges, J.I., Oades, J.M., 1997. Comparative organic geochemistries of soils and marine sediments. Org. Geochem. 27 (7–8), 319–361.
Hostettler, F.D., et al., 1999. A record of hydrocarbon input to San Francisco Bay as traced by biomarker profiles in surface sediment and sediment cores. Mar. Chem. 64 (1–2), 115–127.
Hu, J.F., Peng, P.A., Jia, G.D., Mai, B.X., Zhang, G., 2006. Distribution and sources of organic carbon, nitrogen and their isotopes in sediments of the subtropical Pearl River estuary and adjacent shelf, Southern China. Mar. Chem. 98, 274–285.
Hu, L.M., Guo, Z.G., Feng, J.L., Yang, Z.S., Fang, M., 2009. Distributions and sources of bulk organic matter and aliphatic hydrocarbons in surface sediments of the Bohai Sea, China. Mar. Chem. 113 (3–4), 197–211.
Hu, L.M., et al., 2011a. The role of shelf mud depositional process and large river inputs on the fate of organochlorine pesticides in sediments of the Yellow and East China seas. Geophys. Res. Lett. 38 (3), L03602 http://dx.doi.org/10.1029/2010GL045723.
Hu, L.M., et al., 2011b. Temporal trends of aliphatic and polyaromatic hydrocarbons in the Bohai Sea, China: evidence from the sedimentary record. Org. Geochem. 42 (10), 1181–1193.
Kao, S.J., Lin, F.J., Liu, K.K., 2003. Organic carbon and nitrogen contents and their isotopic compositions in surficial sediments from the East China Sea shelf and the southern Okinawa Trough. Deep Sea Res. Part II 50 (6–7), 1203–1217.
Liu, J.P., et al., 2006. Sedimentary features of the Yangtze River-derived along-shelf clinoform deposit in the East China Sea. Cont. Shelf Res. 26 (17–18), 2141–2156.
Liu, J.P., et al., 2007. Flux and fate of Yangtze River sediment delivered to the East China Sea. Geomorphology 85 (3–4), 208–224.
Mackenzie, A.S., 1984. Applications of biological markers in petroleum geochemistry. In: Brooks, J., Welte, D. (Eds.), Advances in Petroleum Geochemistry, 1. Academic Press, London, pp. 115–214.
McKee, B.A., Aller, R.C., Allison, M.A., Bianchi, T.S., Kineke, G.C., 2004. Transport and transformation of dissolved and particulate materials on continental margins influenced by major rivers: benthic boundary layer and seabed processes. Cont. Shelf Res. 24 (7–8), 899–926.
Meyers, P.A., 1997. Organic geochemical proxies of paleoceanographic, paleolimnlogic, and paleoclimatic processes. Org. Geochem. 27, 213–250.
Milliman, J.D., Shen, H.T., Yang, Z.S., Mead, R.H., 1985. Transport and deposition of river sediment in the Changjiang estuary and adjacent continental shelf. Cont. Shelf Res. 4 (1–2), 37–45.
Müller, P.J., 1977. C/N ratios in Pacific deep-sea sediments: effect of inorganic ammonium and organic nitrogen compounds sorbed by clays. Geochim. Cosmochim. Acta 41 (6), 765–776.
O'Leary, M.H., 1985. Carbon isotope fractionation in plants. Phytochemistry 20, 553–567.
Pancost, R.D., Boot, C.S., 2004. The palaeoclimatic utility of terrestrial biomarkers in marine sediments. Mar. Chem. 92 (1–4), 239–261.
Pang, X., Li, M., Li, S., Jin, Z., 2003. Geochemistry of petroleum systems in the Niuzhuang South Slope of Bohai Bay Basin. Part 2: evidence for significant contribution of mature source rocks to "immature oils" in the Bamianhe field. Org. Geochem. 34 (7), 931–950.
Prahl, F.G., Ertel, J.R., Goni, M.A., Sparrow, M.A., Eversmeyer, B., 1994. Terrestrial organic carbon contributions to sediments on the Washington margin. Geochim. Cosmochim. Acta 58 (14), 3035–3048.
Ramaswamy, V., et al., 2008. Distribution and sources of organic carbon, nitrogen and their isotopic signatures in sediments from the Ayeyarwady (Irrawaddy) continental shelf, northern Andaman Sea. Mar. Chem. 111, 137–150.
Redfield, A.C., Ketchum, B.H., Richards, F.A., 1963. The influence of organisms on the composition of sea water. In: Hill, M.N. (Ed.), The Sea. Wiley, New York, pp. 26–77.
Ruttenberg, K.C., Goñi, M.A., 1997. Phosphorus distribution, C:N:P ratios, and $\delta^{13}C_{oc}$ in arctic, temperate, and tropical coastal sediments: tools for characterizing bulk sedimentary organic matter. Mar. Geol. 139 (1–4), 123–145.
Schubert, C.J., Calvert, S.E., 2001. Nitrogen and carbon isotopic composition of marine and terrestrial organic matter in Arctic Ocean sediments: implications for nutrient utilization and organic matter composition. Deep Sea Res. Part II 48 (3), 789–810.
Showers, W.J., Angle, D.G., 1986. Stable isotopic characterization of organic carbon accumulation on the Amazon continental shelf. Cont. Shelf Res. 6 (1–2), 227–244.
Tan, F.C., Cai, D.L., Edmond, J.M., 1991. Carbon isotope geochemistry of the Changjiang estuary. Estuarine Coastal Shelf Sci. 32 (4), 395–403.
Tesi, T., Miserocchi, S., Goni, M.A., Langone, L., 2007. Source, transport and fate of terrestrial organic carbon on the western Mediterranean Sea, Gulf of Lions, France. Mar. Chem. 105 (1–2), 101–117.
Volkman, J.K., Farrington, J.W., Gagosian, R.B., 1987. Marine and terrigenous lipids in coastal sediments from the Peru upwelling region at 15°S: sterols and triterpene alcohols. Org. Geochem. 11 (6), 463–477.
Volkman, J.K., Holdsworth, D.G., Neill, G.P., Bavor Jr., H.J., 1992. Identification of natural, anthropogenic and petroleum hydrocarbons in aquatic sediments. Sci. Total Environ. 112 (2–3), 203–219.
Wu, Y., et al., 2007. Tracing suspended organic nitrogen from the Yangtze River catchment into the East China Sea. Mar. Chem. 107 (3), 367–377.
Xing, L., Zhang, H., Yuan, Z., Sun, Y., Zhao, M., 2011. Terrestrial and marine biomarker estimates of organic matter sources and distributions in surface sediments from the East China Sea shelf. Cont. Shelf Res. 31 (10), 1106–1115.

Xu, K., Milliman, J.D., 2009. Seasonal variations of sediment discharge from the Yangtze River before and after impoundment of the Three Gorges Dam. Geomorphology 104 (3–4), 276–283.
Yang, Z.S., Guo, Z.G., Wang, Z.X., 1992. Basic pattern of transport of suspended matter from the Yellow Sea and East China Sea to the eastern deep seas. Acta Oceanolog. Sin. 14 (2), 81–90.
Yang, Z.S., et al., 2006. Dam impacts on the Changjiang (Yangtze) River sediment discharge to the sea: The past 55 years and after the Three Gorges Dam. Water Resour. Res. 42, W04407 http://dx.doi.org/10.1029/2005WR003970.
Yang, S.L., Zhang, J., Xu, X.J., 2007. Influence of the Three Gorges Dam on downstream delivery of sediment and its environmental implications, Yangtze River. Geophys. Res. Lett. 34 (10), L10401 http://dx.doi.org/10.1029/2007gl029472.
Yu, F., et al., 2010. Bulk organic $\delta^{13}C$ and C/N as indicators for sediment sources in the Pearl River delta and estuary, southern China. Estuarine Coastal Shelf Sci. 87 (4), 618–630.
Yu, H., Wu, Y., Zhang, J., Deng, B., Zhu, Z., 2011. Impact of extreme drought and the Three Gorges Dam on transport of particulate terrestrial organic carbon in the Changjiang (Yangtze) River. J. Geophys. Res. 116, F04029 http://dx.doi.org/10.1029/2011jf002012.
Zhu, C., et al., 2008. The dispersal of sedimentary terrestrial organic matter in the East China Sea (ECS) as revealed by biomarkers and hydro-chemical characteristics. Org. Geochem. 39 (8), 952–957.
Zhu, C., et al., 2011a. Characterizing the depositional settings for sedimentary organic matter distributions in the Lower Yangtze River—East China Sea Shelf System. Estuarine Coastal Shelf Sci. 93 (3), 182–191.
Zhu, C., et al., 2011b. Sources and distributions of tetraether lipids in surface sediments across a large river-dominated continental margin. Org. Geochem. 42 (4), 376–386.
Zonneveld, K., et al., 2010. Selective preservation of organic matter in marine environments; processes and impact on the sedimentary record. Biogeosciences 7 (2), 483–511.